A computational study of the interaction of oxygenates with the surface of rutile TiO_2(110). Structural and electronic trends

OPEN ACCESS
IOP Publishing
Journal of Physics: Condensed Matter
J. Phys.: Condens. Matter **34** (2022) 154002 (9pp)
https://doi.org/10.1088/1361-648X/ac4d5b

A computational study of the interaction of oxygenates with the surface of rutile TiO_2(110). Structural and electronic trends

C Rohmann[1] **and H Idriss**[2,3,*]

[1] Physical Measurement Laboratory, National Institute of Standards and Technology (NIST), Gaithersburg, MD 20899, United States of America
[2] Institute of Functional Interfaces (IFG), Karlsruhe Institute of Technology (KIT), D-76344 Eggenstein-Leopoldshafen, Germany
[3] Department of Chemistry, University College London, WC1H 0AH, London, United Kingdom

E-mail: hicham.idriss@kit.edu

Received 31 October 2021, revised 27 December 2021
Accepted for publication 20 January 2022
Published 8 February 2022

Abstract

A variety of OH containing molecules in their different modes of adsorption onto the rutile TiO_2(110) are studied by means of density functional theory. A special focus is given to ethanol, ethylene glycol and glycerol. The different species were analyzed with respect to the adsorption energy, work function, and atomic Bader charges. Our results show that dissociated adsorption is favored in all cases. Within these modes, the strongest binding is observed in the case of bidentate fully dissociated adsorption, followed by bidentate partially dissociated then the monodentate dissociated modes. The dependence is also noted upon charge transfer analysis. Species adsorbing with two dissociated OH groups show a negative charge which is roughly twice as large compared to those exhibiting only one dissociated group. In the case of molecular adsorption, we find a small positive charge on the adsorbate. The change in work functions obtained is found to be negative in all studied cases. We observe a trend of the work function change being more negative for glycerol (3 OH groups) followed by ethylene glycol (2 OH groups) and the remaining alcohols (1 OH group), thus indicating that the number of OH groups present is an important factor in regards to work function changes. For the complete series of adsorbates studied (methanol, ethanol, isopropanol, ethylene glycol, glycerol, hydrogen peroxide and formic acid) there is a linear relationship between the change in the work function and the adsorption energy for the molecular adsorption mode. The relationship is less pronounced for the dissociated adsorption mode for the same series.

Keywords: computational, interaction, oxygenates, rutile, TiO_2, structural

Supplementary material for this article is available online

(Some figures may appear in colour only in the online journal)

* Author to whom any correspondence should be addressed.

1. Introduction

The nature of interaction of adsorbates with metal oxides is behind most chemical reactions in nature. The interaction is dominated by both structural and electronic properties of the reactive system (surface/adsorbate). This has attracted a non-negligible work in order to obtain data relevant to understanding many fundamental aspects and concepts including adsorption energy, changes in the work function as well as dipole moments, electronic redistribution and hybridization, surface relaxation, shifts of the Fermi level and bands edges, among others. TiO_2, and in particular the (110) surface of rutile TiO_2, is the most understood metal oxide surface and therefore serves as a prototype for surface interactions and reactions. This understanding is in part a consequence of its stability in ambient conditions, its non-toxicity, and its use in a large number of thermal, photon, and electron driven chemical reactions [1–7].

Finding trends within a family of compounds can provide information related to shift in selectivity of catalytic reactions such as acetylene hydrogenation to ethylene [8], surface poisoning by undesired adsorbates, such as in CO on Pt electrodes [9] or accumulation of non-reactive intermediates that may or may not protect surfaces [10] or enhance catalytic reactions such as in ethylene epoxidation [11]. It can also help in designing the needed surfaces because of the electronic and structural changes imposed on them upon adsorption [12]. While there is a large body of work on the interaction of many different surfaces with a given chemical [13], less work has focused on the effect of the nature of a given surface on the interaction of a large family of adsorbates [14]. There are however common trends and observations that were obtained using both approaches. Focusing on computational results, over TiO_2(110), in general dissociative adsorption of linear alcohols is more favored than molecular adsorption at least in the case of ethanol [15, 16] whereas methanol molecular and dissociative adsorptions are largely iso-energetic and evidence points out to the presence of both on the surface at 300 K [17, 18]. While iso-propanol adsorption on TiO_2(110) has been studied experimentally in good details [19, 20] on the rutile TiO_2(110) we are aware of only one reported PW-density functional theory (DFT) study [21] in which the results tend to agree with the observed relative instability of the molecular form when compared to the dissociative one. This observation has indeed some implications on photo-catalytic reactions. It was observed computationally that the dissociated [15, 16, 22] form has the potential to inject electrons into the valence band (VB) (hole trapping) of TiO_2 because it is much closer to its energy level (mainly composed of O2p). On the contrary, the molecularly adsorbed form has its HOMO further away (lower in energy) and therefore may not inject electrons into the VB [23, 24]. Also, in general the adsorption of oxygen containing compounds (and by analogy their N and S homologues) results in a decrease of the work function and dipole moment of the surface [25–28]. Linked to that are changes in the band gap positions and in particular the conduction band (CB) minimum [29]. Adsorbates structures also changes their properties (coverage effect and change in dipole moment among others) [30–32]; probably the most known example for organic adsorbates is the 2×1 structure of carboxylates on rutile TiO_2(110) surface (maximum coverage is 0.5 ML with respect to five-fold coordinated Ti^{4+} cations) [33, 34]. The adsorbate system becomes more complex when the molecule in question contains more than one heteroatom such as in ethanolamine (NH_2–CH_2CH_2–OH) [35], more than one functional group, such as in glycerol (OH–CH(OH)CH_2–OH) [36] or different functional groups such as in acrolein (CH_2 = CHCH = O) [37]. In these cases, adsorption modes and consequently their effects on the electronic structure are largely dominated by the nature of secondary interactions.

In this work, we have investigated in particular three OH containing molecules in their different modes of adsorption. These are ethanol (CH_3CH_2OH), ethylene glycol (OH–CH_2CH_2–OH), and glycerol (OH–CH_2CH(OH)CH_2–OH). We have also studied a number of molecules outside this family for comparison, these include methanol (to compare with ethanol as it does not have a C–C bond), iso-propanol (a homologue to glycerol, missing the two terminal –OH groups) and H_2O_2 which has a stable bridging adsorption mode [16] but is non-carbon containing compound. To conduct the work, we have used DFT-GGA-PBE because it performs reasonably well for surface adsorbates structures on stoichiometric TiO_2 even if the band edges are narrowed when compared to experimental ones by up to 1.5 eV [38]. We have however, also employed DFT + U ($U = 4.2$ eV) and the hybrid method ((αDFT-GGA + (1 − α) HF), α (mixing parameter) = 0.25.) as implemented in HSE-06 (for comparison in certain cases). Adsorption energy, work function, and atomic Bader charge analysis were studied.

2. Methodology

DFT calculations using the Vienna *Ab initio* Simulation Package (VASP) [39] and the PAW method [40] with the Perdew–Burke–Ernzerhof generalized-gradient approximation (PBE-GGA) functional [41] were employed. All structures were relaxed until the total energy converges to within 10^{-6} eV during the self-consistent loop, with forces converged to 0.01 eV $Å^{-1}$, while employing the Methfessel-Paxton method with a smearing of 0.02 eV width. The energy cut-off and Monkhorst Pack mesh [42] were tested employing the actual cell dimension determined to be feasible (see below) for this study. Test calculations show that an increase from 500 eV to 550 eV or a denser k-mesh, $2 \times 2 \times 1$ vs $3 \times 3 \times 1$ did not change the total energy within 0.01 eV. Thus, the Brillouin zone was sampled with a $2 \times 2 \times 1$ Monkhorst Pack mesh and an energy cut-off of 500 eV was used for all calculations. Van der Waals interactions were accounted for by means of the Grimme (D2) scheme where a correction term is added to the calculation [43]. More sophisticated dispersion correction methods as recently discussed by Rehak *et al* [44] show no or only marginal improvement for molecules adsorbing onto metal oxide surfaces. The valence electron configuration for each atom considered is O:$2s^2 2p^4$, Ti: $2p^6 3d^3 4s^1$ ($3d^3 4s^1$ in case of structural relaxation), C:$2s^2 2p^2$ and H:$1s^1$.

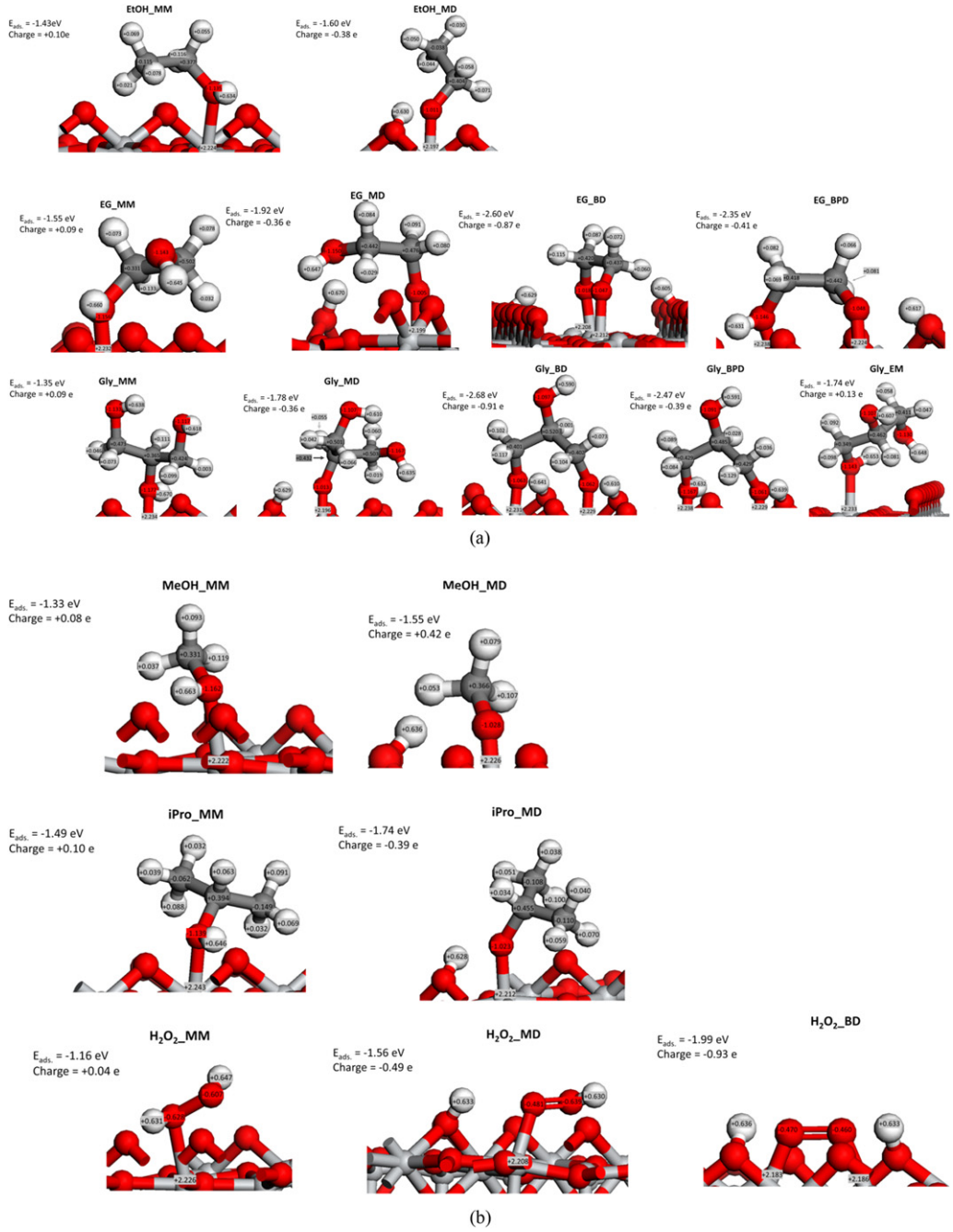

Figure 1. (A) DFT-PBE computed structures, adsorption energies and adsorbate charges of ethanol, ethylene glycol and glycerol, in different configurations, over the rutile $TiO_2(110)$ surface. MM represents monodentate molecular, MD monodentate dissociated, BD bidentate dissociated, BPD bidentate partially dissociated while EM represents the edge monodentate. (B) DFT-PBE computed structures, adsorption energies and adsorbate charges of methanol, isopropanol and hydrogen peroxide, in different configurations, over the rutile $TiO_2(110)$ surface. MM represents monodentate molecular, MD monodentate dissociated, BD bidentate dissociated and BPD represents bidentate partially dissociated. Please note, each mode of adsorption shown was obtained by creating the respective structure manually which was then further optimized.

The work function is calculated by subtraction of the Fermi energy obtained in the OUTCAR file from the vacuum reference potential (mid-point) that was obtained by employing the p4vasp software. The charge on each atom was computed employing the Bader charge analysis [45].

Bulk TiO_2 was cut along the 110 direction at a thickness of 5 stoichiometric layers adding a 22 Å vacuum layer to create the $TiO_2(110)$ surface. In the following, lattice parameters were optimized to $a = 2.964$ Å and $b = 6.569$ Å. The adsorption of the investigated molecules was studied initially at the 2×1 supercell to reduce the computational cost, while finial optimization took place at a 4×2 super cell with dimensions of $a = 11.857$ Å and $b = 13.137$ Å. Test calculations, employing all investigated molecules, shows that further increasing the dimension from those of the 4×2 super cell to $a = 15.000$ Å and $b = 20.000$ Å does not change

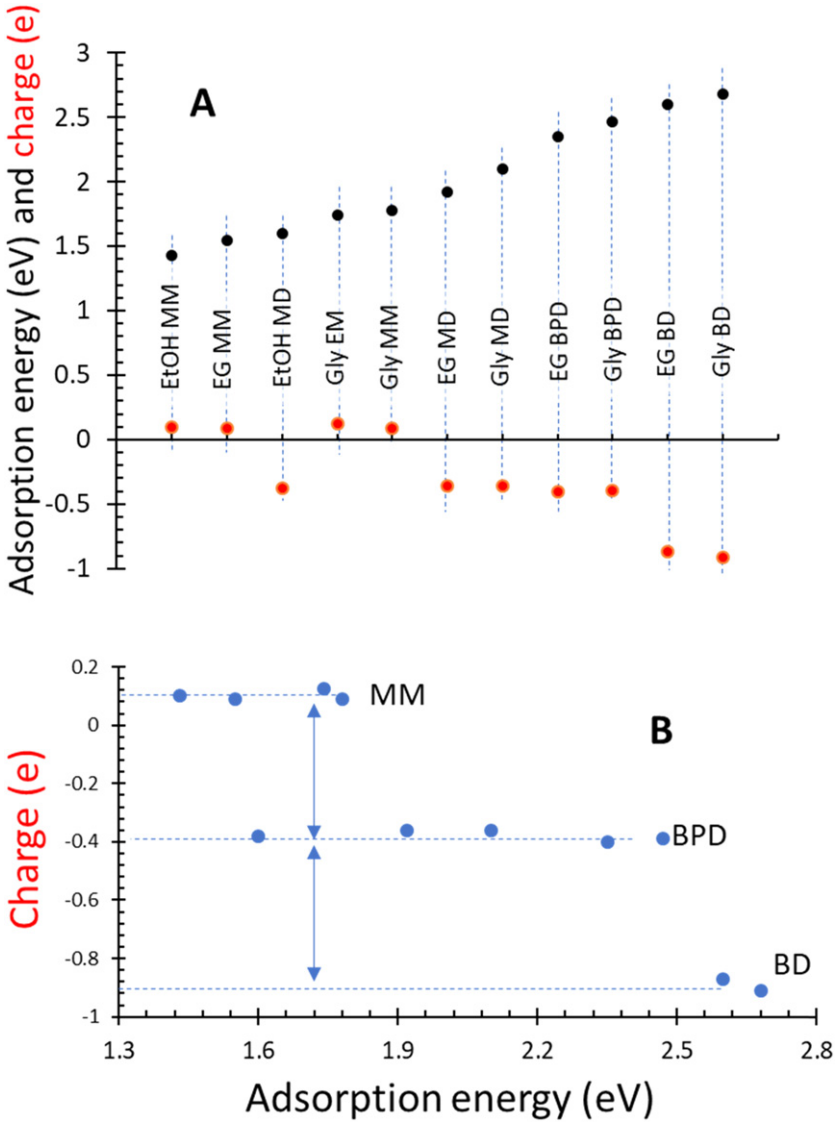

Figure 2. (A) DFT-PBE computed adsorption energies and adsorbate charges for the series containing one, two and three hydroxyl groups over the rutile TiO_2(110) surface. (B) Charge of the adsorbed species in their molecular, partially dissociated and fully dissociated configurations.

the total energy of the isolated molecules (e.g. in case of ethanol it remains at −46.97 eV).

The following molecules were adsorbed to the TiO_2(110): methanol, ethanol, isopropanol, glycerol, ethylene glycol, formic acid and hydrogen peroxide. All species were adsorbed with the O of the OH group facing a fivefold coordinated surface Ti atom. In case of dissociative adsorption, the H being split off was placed within 1 Å of the nearest neighbor twofold coordinated O atom. Adsorption geometries investigated included the monodentate molecular (MM) and monodentate dissociated (MD) arrangement in all cases, while some species were also studied in a bidentate dissociated (BD) and bidentate partially dissociated (BPD) fashion.

The adsorption energy is defined as

$$E_{\text{ads}} = E_{\text{ads+TiO}_2} - \left(E_{\text{M}} + E_{\text{bare TiO}_2}\right) \quad (1)$$

where ads is an abbreviation for adsorbate and M for the free molecule. The coverage of the 4 × 2 surface that contains 8 Ti_{5c} is 1/8 for a monodentate adsorption and 1/4 for a bidentate mode.

3. Results

Figure S1 (https://stacks.iop.org/JPCM/34/154002/mmedia) presents the surface of the rutile TiO_2(110) and the corresponding Bader charges on Ti and O atoms computed by means of DFT, DFT + U (4.2 eV) [46] and HSE06. Although each method has its shortcomings regarding the charge analyses, yet the trend is in line with expectation and previous work [47, 48]. Bridging oxygen atoms have a slightly less negative charge ($-1e$) than the in-plane three-fold oxygen atoms ($-1.1e$). Probably the coordination number is the reason for this, since the in-plane oxygen atoms are in contact

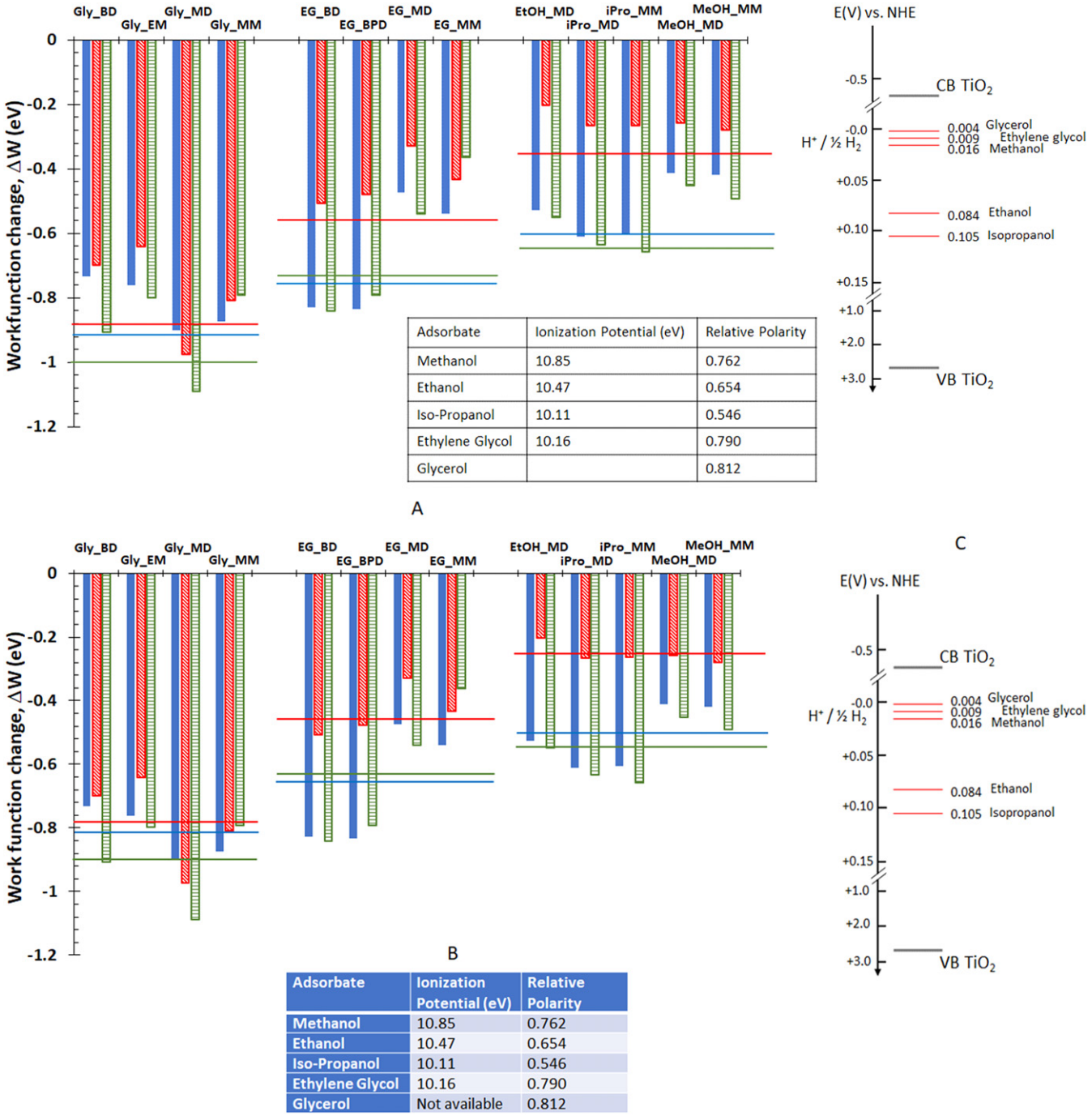

Figure 3. (A) Computed work function changes for the series of adsorbates containing one, two or three hydroxyl groups over the surface of rutile TiO_2(110) using different methods. Blue (solid) for DFT-PBE, Red for DFT + U and Green for HSE-06. The horizontal lines are the average work function change for all modes of adsorption using the three methods. (B) Ionization potential and relative polarity for the series of adsorbates considered in (A) (there are no reported experimental ionization energy for glycerol). (C) Computed redox potential of a series of organic compounds with respect to normal hydrogen electrode [57], $H^+/1/2H_2$, also shown are the valence and CBs of TiO_2.

with three Ti cations while the bridging oxygen atoms are in contact with two Ti cations. No difference is seen between the five- and six-fold coordinated surface Ti cations (+2.3e) and no difference is seen between Ti atoms in the second and first layers. It seems however, that charges are slightly more localized moving from DFT-GGA to DFT + U to HSE-06.

To gauge the modes of adsorption, adsorption energy, and adsorbate charges we have compared those of ethanol, ethylene glycol, and glycerol. The adsorption of oxygen containing compounds, such as alcohols, on stoichiometric metal oxides in general is largely governed by an acid-base type of interaction in which no electron transfer occurs. In this case the interaction is dominated by the electron density around the oxygen atom (the Lewis base site) and empty electronic states of the metal cation of the surface (the Lewis acid site of the surface) [15, 49, 50]. This in its simplest form leads to a molec-

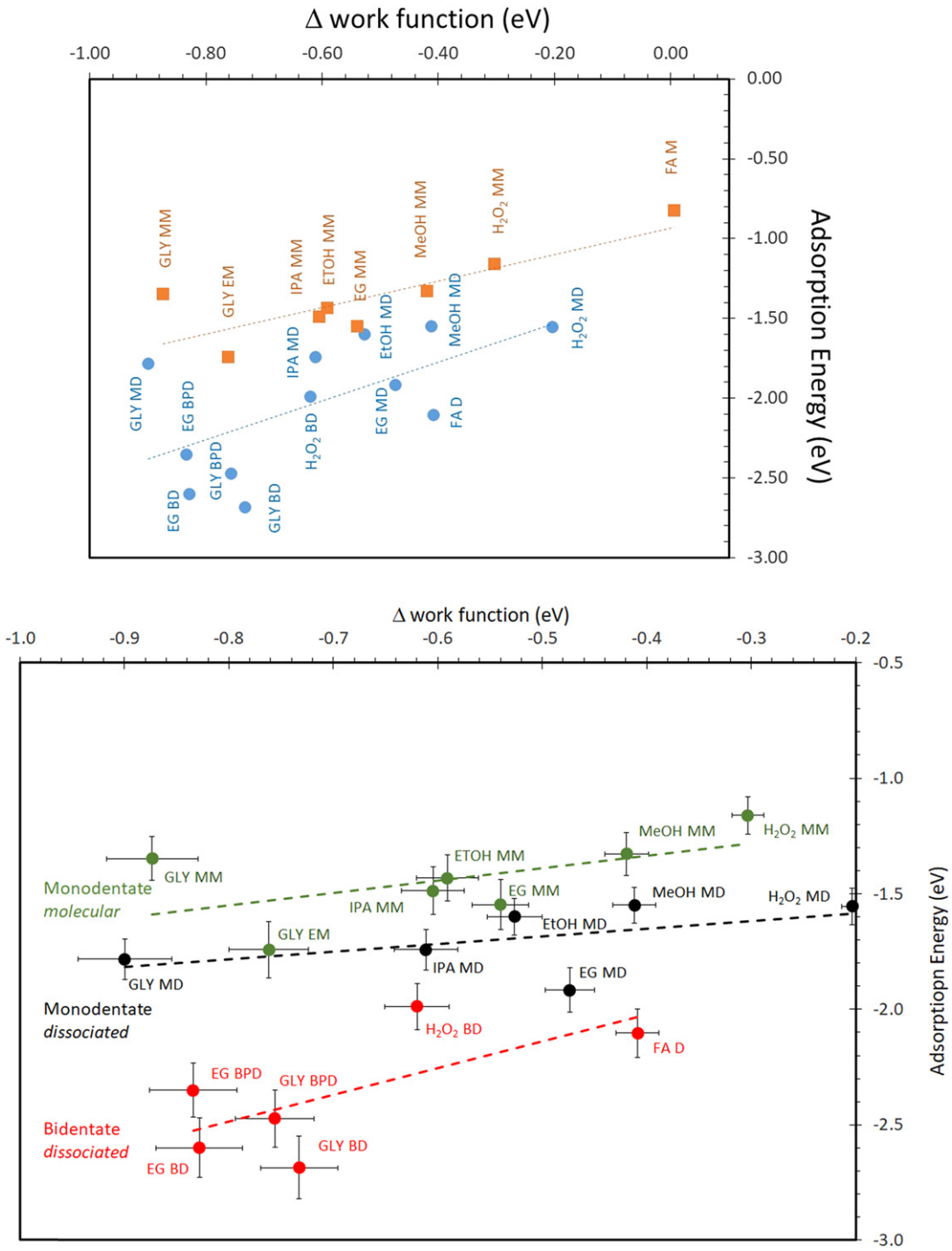

Figure 4. A plot of computed (DFT-PBE) changes in the work function versus the adsorption energy for the series of compounds studied in the different molecular and dissociative adsorption modes; the lines are linear regressions.

ular mode of interaction. All other type of interaction would be very weak. Also, in general the structure is dominated by the shape of the HOMO orbitals of the adsorbed molecule and empty orbitals (states) of the surface atoms (metal cations) [51] and the repulsive nature of the alkyl chain of the adsorbate with the surface. This leads to upright or titled configurations [52]. The three molecules have the hydroxyl groups in common that may dissociate upon adsorption. The presence of multiple hydroxyls allows for bridged configurations in addition which can be dissociative or non-dissociative. Figure 1 presents the different modes of adsorption for these three compounds. Ethanol adsorbed in the molecular form has an energy of −1.43 eV while its dissociative mode is slightly more stable (−1.6 eV). The Bader charge analysis indicates that the molecular mode has a small positive charge which might be due to some loss associated to the O2p interaction with the empty d orbitals of the five-fold coordinated Ti^{4+} cations (Ti_{5c}). A slight decrease in the charge of similar molecules has

also been observed by others [53, 54]. The dissociated mode on the contrary is negatively charged due to the loss of the proton (to protonate the bridging oxygen atom). The molecular adsorption of ethylene glycol is similar to that of ethanol, albeit the adsorption energy is slightly higher (−1.55 eV) and its dissociative mode (in a monodentate structure) is considerably more stable (−1.92 eV). The bidentate modes of adsorption were also investigated. The partially dissociated one has a higher adsorption energy (−2.35 eV) and the fully dissociated bidentate mode was further stabilized (adsorption energy = −2.60 eV). Like ethanol the molecular adsorption resulted in a marginal change of the Bader charge. The partially dissociated modes were both negatively charged (up to $-0.4e$) and the fully dissociated mode was twice as much charged ($-0.87e$). The different modes of adsorption of glycerol are also presented in figure 1. Like ethylene glycol, the molecular mode showed the weakest adsorption energy (about −1.75 eV) with negligible changes in the charge. The adsorption via the terminal or central –OH group (MM vs EM mode) showed virtually no change in both adsorption energy or charge. The bidentate modes were more stable. The most stable mode was the fully dissociated one with the highest adsorption energy found to be equal to −2.68 eV and the charge ($-0.91e$) was very close to that observed for ethylene glycol ($-0.87e$). For a given compound, the distance between the oxygen of the adsorbate and Ti_{5c} tracks the adsorption energy with the shortest distance found for the most stable modes of adsorption, table S1. For example, in the case of ethylene glycol the Ti–O distance was 2.13 and 1.81 Å for the molecular and fully dissociated modes, respectively.

To determine any possible trends, the computed adsorption energies and charges for all modes investigated are presented in figures 2(A) and (B). The increasing adsorption energy from ethanol to glycerol is mostly determined by the overall electronic structure of the molecule and is not connected to the charge. The main contribution of the charge is the dissociative versus molecular adsorption with the former appearing to be additive; the dissociative bidentate mode has a charge twice as large as the monodentate dissociative mode of adsorption. The main reason is the loss of the protons, which also explains the almost identical charges comparing the MD and BPD cases. In these, only one OH group dissociates. The Ti–O bond length also does not give a general trend indication about the magnitude of the adsorption energy; with the exception of the molecular versus dissociative interaction as indicated above. For example, the Ti–O bond length of dissociatively adsorbed ethanol is very close to that of the bidentate glycerol in a dissociative mode yet the adsorption energy difference is about 1 eV (see table S1). Further we have investigated methanol, isopropanol and hydrogen peroxide. We have chosen to study methanol due to its similarities with ethanol and isopropanol because it is structurally homologous to glycerol except that the two terminal -OH groups are absent. We have previously studied H_2O_2 in its different modes and it is here studied to determine similarities, albeit non-carbon containing compound, with regards to the bidentate structural effect [16]. Figure 1(B) presents the structural modes, adsorption energies and charges for these three molecules. The trends observed for these species are all in line with respect to the three alcohols studied earlier. We find the bidentate mode the most stable, with the dissociated monodentate preferred over the molecular mode. The charges also reflect the earlier noted trends of (i) a slightly positive charge of the adsorbate in case of molecular adsorption (ii) all dissociated modes show a notable negative charge (iii) and a roughly doubling of the charge moving from the fully dissociated monodentate mode to the bidentate adsorption mode.

The extraction of the work function changes upon adsorption was conducted next. The work function changes were computed using the three methods mentioned earlier to determine possible variations. To do this we have minimized the structure using DFT-PBE then applied DFT + U and HSE06 on these structures without further minimization. In doing so we may see the effect of the method on the same structure. Figure 3 presents the results of the series of alcohols, ethylene glycol, and glycerol. Changes in the work functions are, as expected, negative since all molecules are electron donating. The magnitude of the work function changes with the method used, yet they seem to be in line with the overall properties of the adsorbates. Three main observations can be extracted from these results. The first observation is that glycerol induces the highest effect on the work function followed by ethylene glycol then by the alcohols, which indicates a relation between the work function and the number of OH groups present. The higher the number of OH groups the more negative is the change in work function. The second observation is that the mode of adsorption has a small effect on changes in work function, this extends further into the dissociative versus molecular mode where no particular effect is seen. Considering that changes in the atomic structure of TiO_2 between a dissociative and non-dissociative mode are very small, then most of the work function change would be related to the adsorbate itself and in this case, there is no *a priori* reason why a molecular adsorption mode would affect the work function differently compared to a dissociative mode. The third observation is related to the method used. While DFT-PBE and HSE06 gave mostly the same results, DFT + U deviated considerably. The lack of differences between DFT-PBE and HSE06, may be expected upon closer inspections of both methods because stoichiometric TiO_2 does not have d electrons, which is the main reason why HF is introduced into the semi-local PBF functional [55]. In HSE, and in order to avoid difficult convergence problems due to long-range HF exchange, a screened Coulomb potential ($1/r$) is introduced (only affecting the exchange part of the exchange correlation potential). This exchange part is arbitrary decomposed into long-range and short-range contributions. The following equation introduces the exchange correlation HSE functional: $E_{xc}^{HSE} = \alpha E_x^{HF,SR}(\omega) + (1-\alpha) E_x^{PBE,SR} + E_x^{PBE,LR} + E_c^{PBE,LR}$; with SR and LR being the short- and long-range contributions of the Coulomb interaction, $\frac{1}{r} = SR + LR = \frac{1-erf(\omega r)}{r} + \frac{erf(\omega r)}{r}$. α (mixing parameter) and ω (screen parameter) are empirically derived as 0.25 and 0.21 $Å^{-1}$, respectively and $E_{xc}^{HSE}, E_x^{HSE}, E_c^{HSE}$, are the exchange–correlation, exchange and correlation energies respectively. It is to be noted that the long-range interaction of the HF is not included and when ω goes to infinity HSE

becomes PBE (the erf(ωr) $\rightarrow$ 1) [56]. In other words, probably a non-negligible effect of the changes induced by these OH groups of the organic adsorbate are of a long range. As this is not considered in the mixing, the use of HSE06 in this case may not be needed, or at least does not affect the overall electronic interaction. Another point to mention (and unlike in the case of the PBE and HSE06 methods), the magnitude of deviation when employing DFT + U seems to be related to the number of OH groups in the molecules. In this case the work function changes appear to be directly linked to the number of OH groups (the center of the electron donating in the adsorbates). While the three methods performed similarly in the case of glycerol, changes investigated by DFT + U were smaller in the case of ethylene glycol and became considerably smaller for all alcohols investigated. In other words, the presence of more hydroxyl groups was more tracked using DFT + U.

We are not aware of any systematic experimental studies conducting work function measurements for the series investigated and therefore it is not clear if DFT + U is more accurate or the outliner. In a discussion on the effect of the $+U$ parameter [58] on systems related to catalysis [59] it was indicated that the energy correction ($+U$) depends exclusively on an occupation matrix, sensitive to electron configuration, in other words dependent on the chemical bonding. If there is some overstabilization of the PBE (and probably HSE06 considering the above argument) the $+U$ parameter may correct this. This is because the $+U$ potential is linear in the occupations of the orbitals to which it is applied. Subsequently it is argued that the $+U$ parameter might tune the effective electronegativity of both substituent atoms (in our case the O atoms of the hydroxyls) and the overall molecule.

Furthermore, the decrease in the work function does not seem to be related to the redox potential of these adsorbates. For example, methanol and ethylene glycol have similar redox potentials yet the latter induced twice as much changes in the work function. Similarly, the redox potential of isopropanol is lower than that of methanol with respect to the CB of TiO_2 yet, it causes larger changes in the work function. In addition, the change in work function also do not seem to be related to the ionization potential of the adsorbates either. For example, isopropanol and ethylene glycol have the same ionization potential (10.2 eV). The polarity of the adsorbates also seems not related to the work function since methanol and ethylene glycol have almost the same relative polarity. Closer inspection of the adsorbate structures in figure 1 shows that there is a non-negligible secondary interaction with the other OH groups in the case of ethylene glycol and glycerol and this might be the cause due to their high electron density which may have long range induction into the surface. To gauge this, the average changes of the different adsorbate structures for a given molecule was computed. These are plotted as horizontal lines in figure 3 for the three different methods. If we attribute the changes to be largely related to the number of OH groups, it seems that DFT + U performs best since the changes are tracked best employing this method.

A last correlation is plotted in figure 4 which presents the relationship between the adsorption energy and the changes in work function for the complete series, including formic acid, isopropanol, and hydrogen peroxide. One can observe a trend, in general the higher the adsorption energy of a molecule the larger is the change in the work function. However, one needs to distinguish between molecular and dissociative modes because in most of these compounds the dissociative adsorption mode prevails (highest adsorption energy). It is however clear, that once a given molecule is dissociated its mode of adsorption (structural differences) has a far more effect on the adsorption energy and far less on the work function changes.

4. Conclusions

We have analyzed adsorption energy, work function, and atomic Bader charges of OH containing molecules in their different modes of adsorption onto rutile TiO_2(110) with a special focus on ethanol, ethylene glycol and glycerol. Results show a strong preference of bidentate over monodentate binding, which is weakened only if the respective OH groups do not fully dissociate. The overall trend in regards to the binding strength is BD > BPD > MD > MM. Furthermore, the Bader charge analysis reveals that adsorbate having two or more OH groups present and as such are able to form BD structures, show a significant larger negative charge which is roughly twice as much compared to the BPD or MD modes. The MM mode on the other hand shows a small positive charge. It is interesting to note, that the adsorption mode seems to be the main contributor rather than the structure itself for the changes in the charge, since all structures show similar values for the respective adsorption mode. The analysis of the work function is less clear due to the different methods employed; however, a negative value is obtained in every case. Yet, we also note the influence of the number of OH groups present. In general, a trend in terms of the number of OH groups on a given molecule is seen; most negative for glycerol (3 OH groups) followed by ethylene glycol (2 OH groups) and the remaining alcohols having one OH group is the least.

Acknowledgments

CR and HI acknowledge the initial contribution of Hamdan Al-Ghamdi in performing preliminary structural minimization employing DFT-PBE.

Data availability statement

The data that support the findings of this study are available upon reasonable request from the authors.

ORCID iDs

H Idriss https://orcid.org/0000-0001-8614-7019

References

[1] Schneider J, Matsuoka M, Takeuchi M, Zhang J, Horiuchi Y, Anpo M and Bahnemann D W 2014 *Chem. Rev.* **114** 9919–86
[2] Fujishima A, Zhang X and Tryk D 2008 *Surf. Sci. Rep.* **63** 515–82
[3] Connelly K A and Idriss H 2012 *Green Chem.* **14** 260–80
[4] Bagheri S, Julkapli N M and Hami S B A 2014 *Sci. World J.* **2014** 727496
[5] Wu L, Fu C and Huang W 2020 *Phys. Chem. Chem. Phys.* **22** 9875–909
[6] Liu L and Corma A 2021 *Nat. Rev. Chem.* **5** 256–76
[7] Lačnjevac U *et al* 2020 *J. Mater. Chem.* A **8** 22773–90
[8] Li Q, Wang Y, Skoptsov G and Hu J 2019 *Ind. Eng. Chem. Res.* **58** 20620–9
[9] Chung D Y, Kim H-i, Chung Y-H, Lee M J, Yoo S J, Bokare A D, Choi W and Sung Y-E 2014 *Sci. Rep.* **4** 7450
[10] Li M, Jin Z-X, Zhang W, Bai Y-H, Cao Y-Q, Li W-M, Wu D and Li A-D 2019 *Sci. Rep.* **9** 10438
[11] Pu T, Tian H, Ford M E, Rangarajan S and Wachs I E 2019 *ACS Catal.* **9** 10727–50
[12] Otero R, Vázquez de Parga A L and Gallego J M 2017 *Surf. Sci. Rep.* **72** 105–45
[13] Idriss H and Barteau M A 2000 *Adv. Catal.* **45** 261–331
[14] Tillotson M J, Brett P M, Bennett R A and Grau-Crespo R 2015 *Surf. Sci.* **632** 142–53
[15] Muir J N, Choi Y and Idriss H 2012 *Phys. Chem. Chem. Phys.* **14** 11910–9
[16] Alghamdi H and Idriss H 2018 *Surf. Sci.* **669** 103–13
[17] Zhao J, Yang J and Petek H 2009 *Phys. Rev.* B **80** 235416
[18] Liu S, Liu A-a, Wen B, Zhang R, Zhou C, Liu L-M and Ren Z 2015 *J. Phys. Chem. Lett.* **6** 3327–34
[19] Kim Y K, Kay B D, White J M and Dohnálek Z 2008 *Surf. Sci.* **602** 511–6
[20] Brinkley D and Engel T 2000 *J. Phys. Chem.* B **104** 9836–41
[21] Carchini G and López N 2014 *Phys. Chem. Chem. Phys.* **16** 14750–60
[22] Di Valentin C and Fittipaldi D 2013 *J. Phys. Chem. Lett.* **4** 1901–6
[23] Chu W, Saidi W A, Zheng Q, Xie Y, Lan Z, Prezhdo O V, Petek H and Zhao J 2016 *J. Am. Chem. Soc.* **138** 13740–9
[24] Migani A, Mowbray D J, Iacomino A, Zhao J, Petek H and Rubio A 2013 *J. Am. Chem. Soc.* **135** 11429–32
[25] Marques H P, Canário A R, Moutinho A M C and Teodoro O M N D 2008 *Vacuum* **82** 1425–7
[26] Leung T-C, Hu H, Liu A J and Lin M-C 2019 *Phys. Chem. Chem. Phys.* **21** 25763–72
[27] Rusu P C and Brocks G 2006 *J. Phys. Chem.* B **110** 22628–34
[28] Gossenberger F, Roman T, Forster-Tonigold K and Groß A 2014 *Beilstein J. Nanotechnol.* **5** 152–61
[29] Zapol P and Curtiss L A 2007 *J. Comput. Theor. Nanosci.* **4** 222–30
[30] Ramalho J P P, Illas F and Gomes J R B 2017 *Phys. Chem. Chem. Phys.* **19** 2487–94
[31] Adachi Y, Sugawara Y and Li Y J 2021 *Nano Res.* **15** 1909–15
[32] Reticcioli M, Sokolović I, Schmid M, Diebold U, Setvin M and Franchini C 2019 *Phys. Rev. Lett.* **122** 016805
[33] Heckel W, Würger T, Müller S and Feldbauer G 2017 *J. Phys. Chem.* C **121** 17207–14
[34] Martsinovich N, Jones D R and Troisi A 2010 *J. Phys. Chem.* C **114** 22659–70
[35] Sohn S-D, Kim S H, Kwak S K and Shin H-J 2019 *Appl. Surf. Sci.* **467–468** 1213–8
[36] Babaei Z, Chermahini A N and Dinari M 2020 *J. Colloid Interface Sci.* **563** 1–7
[37] Sherrill A B, Idriss H, Barteau M A and Chen J G 2003 *Catal. Today* **85** 321–31
[38] Labat F, Baranek P, Domain C, Minot C and Adamo C 2007 *J. Chem. Phys.* **126** 154703
[39] Kresse G and Furthmüller J 1996 *Phys. Rev.* B **54** 11169–86
[40] Kresse G and Joubert D 1999 *Phys. Rev.* B **59** 1758–75
[41] Perdew J P, Burke K and Ernzerhof M 1996 *Phys. Rev. Lett.* **77** 3865–8
[42] Monkhorst H J and Pack J D 1976 *Phys. Rev.* B **13** 5188–92
[43] Grimme S 2006 *J. Comput. Chem.* **27** 1787–99
[44] Rehak F R, Piccini G, Alessio M and Sauer J 2020 *Phys. Chem. Chem. Phys.* **22** 7577
[45] Tang W, Sanville E and Henkelman G 2009 *J. Phys.: Condens. Matter* **21** 084204
[46] Yoo S-H, Siemer N, Todorova M, Marx D and Neugebauer J 2019 *J. Phys. Chem.* C **123** 5495–506
[47] Nehaoua N, Belkada R, Tala-Ighil R Z, Thomas L, Chemam R and Mekki D E 2019 *Mater. Res. Express* **6** 025510
[48] Liu R, Zhou X, Yang F and Yu Y 2014 *Appl. Surf. Sci.* **319** 50–9
[49] Calatayud M, Markovits A, Menetrey M, Mguig B and Minot C 2003 *Catal. Today* **85** 125–43
[50] Tang M, Zhang Z and Ge Q 2016 *Catal. Today* **274** 103–8
[51] McGill P R and Idriss H 2008 *Langmuir* **24** 97–104
[52] Muir J M R and Idriss H 2013 *Chem. Phys. Lett.* **572** 125–9
[53] Lupan O *et al* 2021 *Nano Energy* **88** 106241
[54] Liu Y, Zhou W, Sun L, Liang Y and Wu P 2016 *Comput. Mater. Sci.* **121** 174–81
[55] Krukau A V, Vydrov O A, Izmaylov A F and Scuseria G E 2006 *J. Chem. Phys.* **125** 224106
[56] Viñes F, Lamiel-García O, Ko K C, Lee J Y and Illas F 2017 *J. Comput. Chem.* **38** 781–9
[57] Al-Azri Z H N, Chen W-T, Chan A, Jovic V, Ina T, Idriss H and Waterhouse G I N 2015 *J. Catal.* **329** 355–67
[58] Kulik H J 2015 *J. Chem. Phys.* **142** 240901
[59] Lutfalla S, Shapovalov V and Bell A T 2011 *J. Chem. Theory Comput.* **7** 2218–23